Available online at www.sciencedirect.com
SCIENCE DIRECT®
Earth and Planetary Science Letters 248 (2006) 411–425
EPSL
www.elsevier.com/locate/epsl

Small-scale lateral variations in azimuthally anisotropic D″ structure beneath the Cocos Plate

Juliana M. Rokosky [a,*], Thorne Lay [a], Edward J. Garnero [b]

[a] Earth Sciences Department, University of California Santa Cruz, Santa Cruz, CA 95064, USA
[b] Department of Geological Sciences, Arizona State University, Tempe, AZ 85287, USA

Received 30 November 2005; received in revised form 3 June 2006; accepted 3 June 2006
Available online 13 July 2006

Abstract

Shear waves from intermediate and deep focus South American events recorded by California broadband seismometers reveal complex anisotropy in the lowermost mantle. ScS waves densely sample the D″ region beneath the Cocos Plate, just west of Central America (1–16°N; 267–277°E). Our data show evidence for significant near-source anisotropy, which we constrain for each event by performing polarization analyses on an expanded dataset of S waveforms. ScS waveforms are corrected for upper mantle and near-source anisotropy, and estimates of D″ anisotropy are made using the covariance method. We find splits between fast and slow components of ScS ranging from 0.4 to 2.5 s, with an average of 1.6 s. Fast polarization directions in the southern portion of our study area are approximately orthogonal to the raypaths. North of 7° latitude there is a rapid change in fast polarization direction to nearly raypath parallel. Beyond 10° latitude fast directions are more highly scattered than in southern regions. Past work in the region has inferred strong lateral variations in shear wave velocity, but fairly uniform transverse isotropy. In contrast, our results indicate that the lowermost mantle beneath the Cocos plate has azimuthal anisotropy that varies laterally over scales of 100–200 km. In addition, our data suggest connections between previously imaged topography on the D″ discontinuity and the character of anisotropy.

Keywords: core–mantle boundary; anisotropy; shear waves; D″

1. Introduction

After decades of seismological studies, the dynamics of the lowermost mantle are gradually being characterized. Recent work suggests that the region is host to acute shear velocity heterogeneity and intense variability in the strength and topography of the shear velocity discontinuity at the top of the D″ region [1]. Some areas show strong evidence for an ultra-low velocity zone (ULVZ) at the base of D″, potentially signaling the presence of partial melt, while other areas appear to lack such a layer [2]. Determining the key mechanisms active in this region remains challenging, and relating seismological observations to dynamical models and mineral physics observations and calculations is a crucial step toward achieving a better understanding of D″ (e.g. [2,3]).

One promising avenue is the study of seismic wave anisotropy in D″. As has long been clear in studies of the crust and upper mantle, anisotropy can provide key information about deformation and mineralogy (e.g. [4,5]). Characterizing the existence and nature of anisotropy in the lowermost mantle may offer

* Corresponding author.
E-mail address: jrokosky@pmc.ucsc.edu (J.M. Rokosky).

0012-821X/$ - see front matter © 2006 Elsevier B.V. All rights reserved.
doi:10.1016/j.epsl.2006.06.005

constraints on the processes at work in the boundary layer and the scale lengths on which they vary. The value of characterizing D″ anisotropy has been recognized for over a decade and a cadre of possible mechanisms for inducing anisotropy in the lowermost mantle have been proposed (e.g. [6–10]).

In general, observations of D″ properties have been discussed in two end-member models based on apparent distinctions between relatively high and low shear velocity regimes of D″. Most high shear velocity regions (e.g., beneath the Caribbean, Alaska, and N. Siberia) have pronounced shear wave discontinuities at the top of D″ and exhibit shear wave splitting consistent with a relatively homogeneous anisotropic layer that has shear velocity for horizontal particle motion (V_{SH}) elevated several percent relative to the velocity of vertical particle motion (V_{SV}). After upper mantle correction, nearly vertically traveling SKS waves appear to show minimal splitting, consistent with such a model of vertical transverse isotropy in D″ (VTI) [11]. Because high-velocity regions generally underlie zones of past subduction, most explanations for D″ anisotropy involve slabs impinging on the core–mantle boundary (CMB). Downwelling slabs could produce lattice preferred orientation (LPO) in constituent minerals or highly laminated structures, both of which could be consistent with VTI (e.g. [12,13]). Relatively low temperatures in such regions could allow the post-perovskite phase to be present in D″, accounting for the discontinuity [14,15]. Additionally, the anisotropic properties of post-perovskite may be distinct from those of the overlying perovskite [16,17]. In contrast, relatively low shear velocity regions of D″ (e.g., beneath the central and southern Pacific and beneath Africa) exhibit more variable shear wave splitting consistent with isotropy or azimuthal anisotropy [18,19]. Patches of material with $V_{SV} > V_{SH}$ make these regions distinct from the high V_{SH} realms beneath the circum Pacific. The possibility of partial melt in these low velocity regions, which are commonly underlain by extensive ULVZs, suggests that anisotropy there may be best explained by partial melt aligned by boundary layer flow, i.e., shape preferred orientation (SPO). The relatively low velocities suggest that post-perovskite may not occur in these regions because they are too warm, although in some places, such as the central Pacific, a D″ discontinuity has been observed [20]. Regions of D″ exhibiting deep mantle structure transitioning from high to low shear velocity (e.g., beneath the central Atlantic) appear to have minimal anisotropy [21], further strengthening the idea that distinct mechanisms produce anisotropy in high and low velocity regions.

This end-member characterization of D″ anisotropy is undoubtedly an oversimplification and recent work has etched away at the strong distinctions between high and low velocity regions, by suggesting that some high velocity regions have azimuthal anisotropy rather than VTI [22,23]. Generally speaking, the difficulty in isolating D″ anisotropy from the effects of the upper mantle, along with the poor azimuthal coverage plaguing all studies of D″, limit our ability to confidently infer distinctions between the nature and mechanism of anisotropy in high and low shear velocity regions of D″. High-resolution studies sampling a variety of D″ regions with uniform methodology will be necessary to produce a clear picture of the relationship between velocity heterogeneity and anisotropic structure.

In order to place significant constraints on the mechanisms responsible for the lowermost mantle anisotropy we must ascertain the scale lengths over which anisotropic fabric varies both laterally and with depth. The density of data sampling in the lowermost mantle beneath the Cocos plate, west of Central America, makes it an attractive region in which to study D″. Previous high-resolution work in the region has suggested that it is characterized by relatively homogenous VTI material with V_{SH} elevated by nearly 2% relative to V_{SV} [24,25]. Recent work on a broader region of D″ beneath the Caribbean [22,23] suggests that shear wave splitting is not fully explained by VTI, and is more appropriately modeled by tilted transverse isotropy (TTI), a form of azimuthal anisotropy. In addition, studies characterizing the shear wave discontinuity under the Cocos suggest significant lateral variability in the region [26], hinting at the possibility of more complex patterns of anisotropy, if the discontinuity and anisotropy are indeed dynamically linked. Although many data sampling D″ beneath the Cocos plate show clear separation of SH and SV waveforms, some records do show evidence of coupling, motivating us to consider the presence of azimuthal anisotropy. Additionally, past work in the region has failed to consider the impact of near-source anisotropy, which regional studies suggest may be significant [29,30]. Failing to take into account the effects of anisotropy on other parts of the raypath could strongly bias results (Fig. 1) by mis-mapping effects of shallow anisotropy into the lowermost mantle. Wookey et al. [31] investigated D″ anisotropy beneath the northern Pacific using Tonga–Fiji events and found it necessary to make source corrections for their data. In

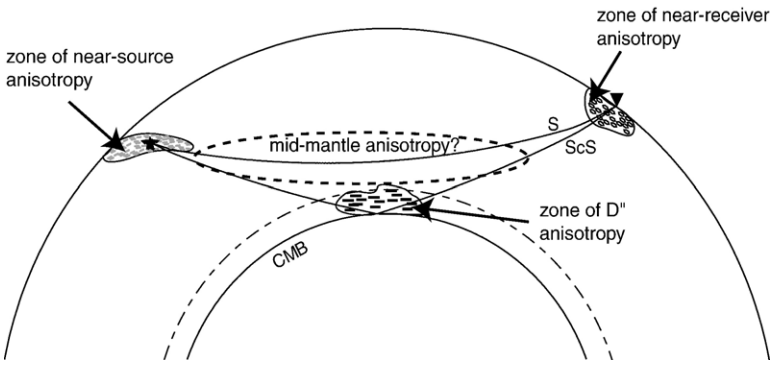

Fig. 1. S and ScS raypaths from a deep source (star) to a receiver (inverted triangle) at teleseismic distance (78°). Shear wave anisotropy may be encountered near the source, near the receiver, in the mid-mantle, or near the base of the mantle. It is generally assumed that mid-mantle anisotropy is minor. Near-source anisotropy is generally neglected for deep focus events.

this study we analyze anisotropy in D″ beneath the Cocos using South American events and also find evidence for near-source anisotropy. We use a similar technique to Ref. [31] in order to take into account both near-source and near-receiver anisotropy. The method used will be useful in characterizing anisotropy in other regions of D″.

2. Data and processing

Our data include records from 13 intermediate and deep focus South American earthquakes recorded by 46 Californian broadband stations [Fig. 2, Table 1]. Epicentral distances for these data range from 65–80°, with ScS paths sampling D″ beneath the Cocos Plate, west of Central America (1–16°N; 267–277°E). We use records of our events from 76 additional North American stations (see inset of Fig. 2), to help assess near-source anisotropy. Events were chosen based on having clear impulsive source–time functions and high signal to noise ratios. All seismograms are deconvolved by the instrument response to produce displacement waveforms (see Fig. 3 for processing steps).

We correct records for previously determined estimates of upper mantle anisotropy [32–35]. These characterizations of near-receiver anisotropy are predominantly based on SKS arrivals, which have smaller incidence angles than the S and ScS arrivals used in our study. Under the conventional assumption of horizontal hexagonal symmetry axis, for the 10° differences in incidence angle typical of SKS and ScS at relevant ranges, the predicted differences in splitting parameters are at most a few tenths of a second and a few degrees in fast direction azimuth. However, if anisotropy actually involves dipping or multiple layers, the characterization of upper mantle anisotropy may vary significantly for different phases (i.e., incident angles). Unfortunately few studies have sufficient data sampling to uniquely constrain the anisotropic orientation [36–38]. Models of upper mantle anisotropy for our stations are not perfectly constrained, but do show consistent regional patterns that suggest the effects are well-approximated to the first-order. Stations with layered models of upper mantle anisotropy tend to have more complex waveforms and few observations for them are retained in our data set. We apply the splitting parameters as reported in the literature to the entire waveform; tests assuming horizontal hexagonal symmetry predict negligible changes in direction and splitting within our waveforms.

Following the corrections for upper mantle anisotropy, significant splitting often remains in the S arrival, as has been noted in previous studies [24,39]. If the two main reservoirs of anisotropy are indeed the upper and lowermost mantle, we would expect S waves from deep earthquakes, which travel through the mid-mantle, to be sensitive only to splitting near the receiver (Fig. 1). The observation of non-linear S motion after upper-mantle corrections could be the result of: (1) inaccuracies in upper mantle anisotropy corrections; (2) anisotropy near the source; or (3) anisotropy in the mid-mantle. As discussed above, upper mantle corrections may have errors associated with them. However, the residual splitting of S is often quite different than can be accounted for by the small changes in the upper mantle correction expected for anisotropy with low degree symmetry systems. Instead the residual splitting tends to be somewhat consistent between sources, suggesting a common origin (see Supplemental Fig. 1 in the Appendix).

Studies of near-slab anisotropy beneath the Nazca Plate [29,30] reveal significant trench parallel anisotropy

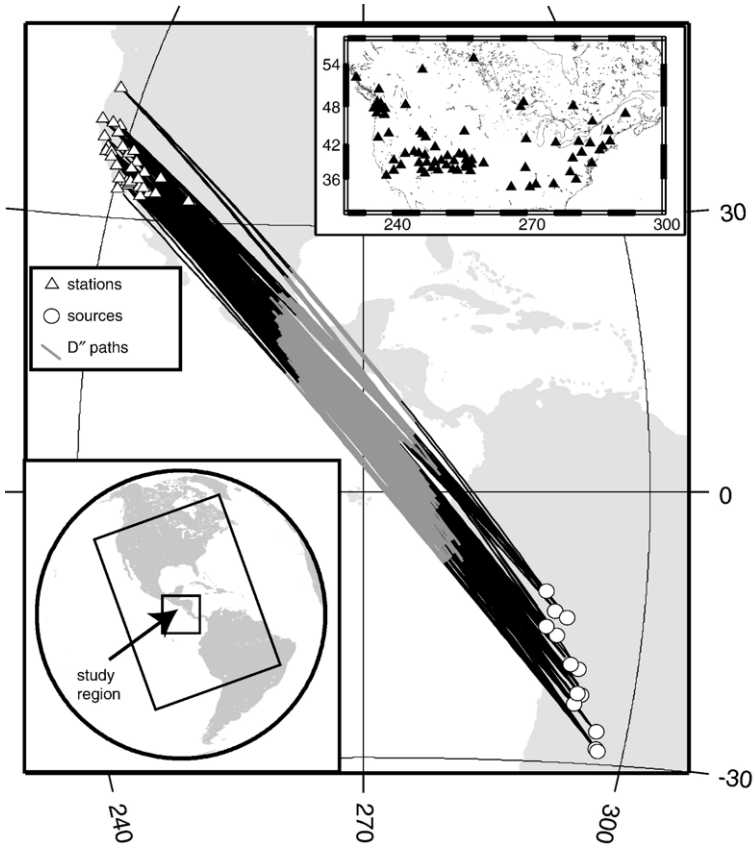

Fig. 2. Map showing the source and station locations with great circle paths, highlighting the portion of the ScS paths within a 300 km thick D″ region. Top right inset shows additional stations used to constrain the residual splitting on S arrivals. The bottom left inset shows the location of the study area map in Fig. 8.

beneath the slab, suggesting that near-source anisotropy may be contributing to the splitting of our S and ScS arrivals. In past studies of lowermost mantle anisotropy, the possibility of near-source anisotropy has usually been addressed by limiting the analysis to deep focus events. However, the assumption that near-source anisotropy is negligible for these deeper events may not be appropriate. In addition, because our data set includes intermediate focus events (200–400 km), the likelihood that near-source anisotropy is affecting at least some of our arrivals is high. We have developed a strategy for estimating and correcting for near-source anisotropy, which will be discussed in detail below. The final possibility for contamination is anisotropy in the mid-mantle. Although, it has been suggested that the transition zone and uppermost lower mantle might harbor some anisotropic fabric [40–42], the bulk of the lower mantle is commonly assumed to be isotropic [11]. We assume that mid-mantle anisotropy is negligible, acknowledging that this is not demonstrated for our data. If there is mid-mantle anisotropy we expect both S and ScS to be affected, but the likelihood that correction by the S splitting will account for the ScS effect is lower than if there is near-source contamination.

Table 1
List of events used in this study

Event date (mm/dd/yy)	Origin time (hh:mm:ss)	Lat (°)	Long (°)	Depth (km)
10/17/90	14:30:15	−10.97	−70.78	598
10/19/93	4:02:22	−22.38	−65.97	272
1/10/94	15:53:50	−13.34	−69.45	596
4/29/94	7:11:30	−28.3	−63.25	561
8/19/94	10:02:51	−26.64	−63.42	563
1/23/97	2:25:22	−27	−65.72	276
7/20/97	10:14:22	−22.98	−66.3	256
9/15/99	3:01:24	−20.93	−67.28	218
4/23/00	17:01:17	−28.31	−62.94	609
5/12/00	18:43:23	−23.55	−66.45	225
10/12/02	20:09:11	−8.27	−71.69	532
7/27/03	11:41:27	−20.14	−65.13	347
3/17/04	3:21:07	−21.12	−65.586	289

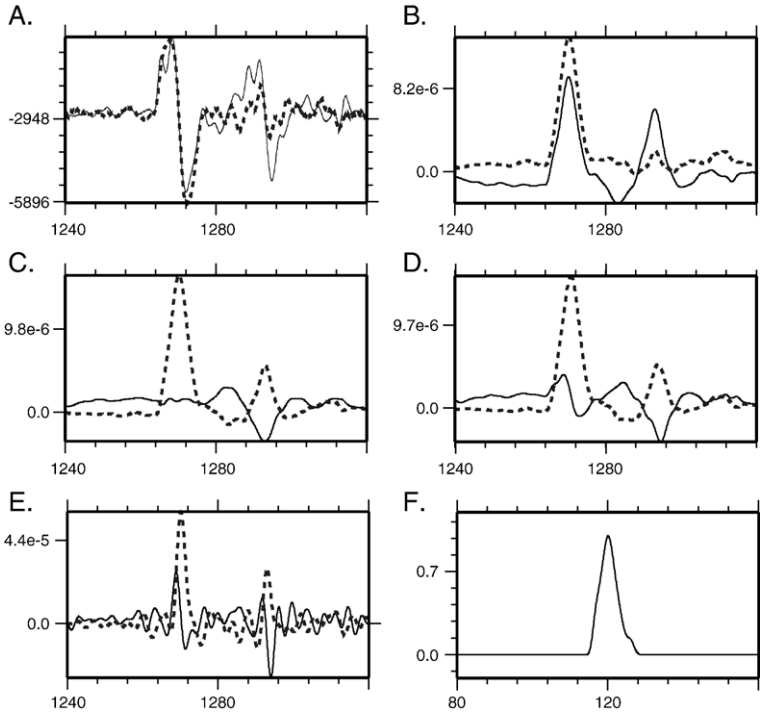

Fig. 3. Steps in processing data. A. Original seismograms in digital counts; N–S component is dotted, E–W is solid line. B. Seismograms deconvolved to restore ground displacements in m. C. Rotated to great circle path. Radial component is solid line; transverse dotted. D. Receiver corrected records. On waveforms used in ScS analysis a small shift is also made for the SV advance at the core. E. Waveforms deconvolved by the source wavelet. F. Source wavelet used in this deconvolution.

After applying upper mantle corrections, waveforms are corrected for a small advance (0.24 s) of ScSV at the core–mantle boundary. This shift varies slowly with distance, but more specific correction requires precise knowledge of velocity gradients at the CMB [39]. In general, this correction is too small to affect our splitting results. Waveforms for each event are deconvolved by an average source wavelet obtained by stacking transverse component ScS arrivals. Source wavelet deconvolution equalizes the signals between events and improves the temporal resolution of arrivals. The narrower pulses that result from deconvolution generally yield more robust splitting measurements, but our work indicates that the splitting measurements are consistent between displacement and deconvolved traces for high quality events.

Before measuring splitting parameters for ScS, we estimate the potential contribution of near-source anisotropy. We use the covariance method [43] to find the fast direction and delay time that best linearizes each S arrival (Fig. 4) after applying receiver corrections. Our S observations are from North American stations only, given the very limited azimuthal coverage for broadband recordings of S waves from deep South American events. The requirement of stable SV and SH signals further limits the number of useable observations. The quality of these results is assessed using the following criteria: (1) Linearity of the final corrected waveform; (2) The similarity of fast and slow waveforms; (3) The magnitude of error bars on the fast azimuth and delay time values as calculated using an inverse F test; (4) The isolation of the second eigenvalue (lambda 2) minimum, e.g. if second eigenvalues are small (waveforms are nearly linear) for all angles and delay times the result is down-weighted. The correspondence between predicted initial polarization and the polarization of corrected waveforms can also be used to assess the quality of results,. Although the polarizations of our corrected waveforms are generally close to the initial polarizations predicted with Harvard CMT focal mechanisms (e.g. [44]), we do not use this as a strong weighting factor in our quality assessment because of uncertainty in the focal mechanisms.

We assign each record a quality grade of A, B, or C. Records of A quality are highly linear after correction, have similar fast and slow waveforms, low errors and well-isolated lambda 2 minima. B quality records fail one of the above criteria, but are generally robust. C

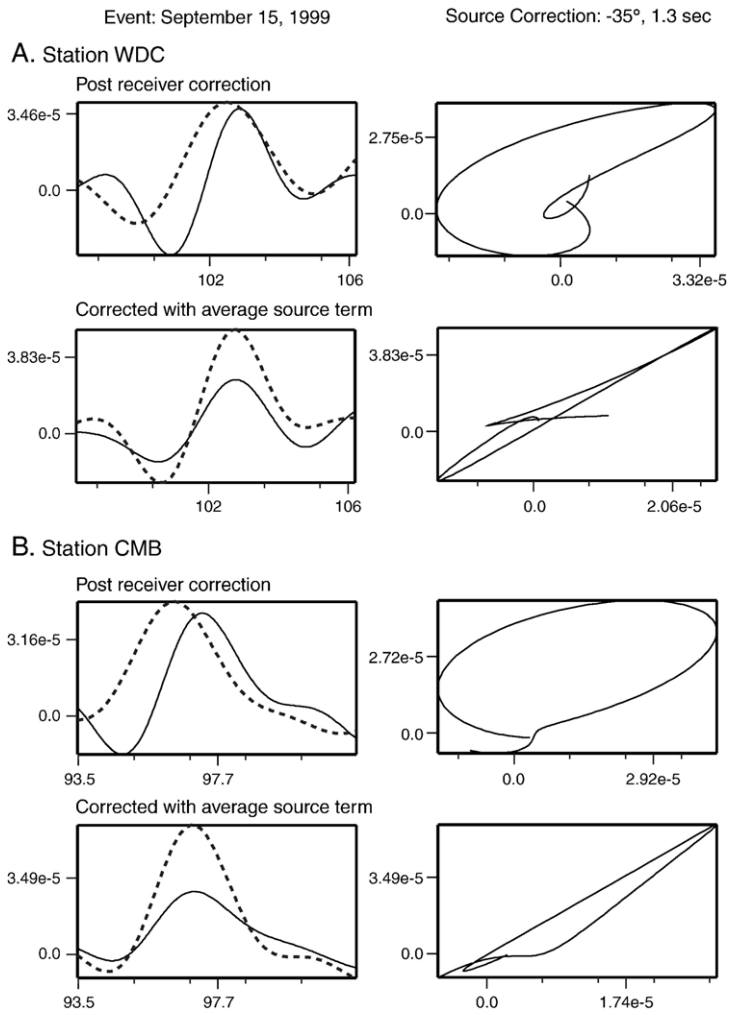

Fig. 4. S arrivals at two stations for the September 15, 1999 event. Records are shown after receiver corrections and following correction with average source term for the event. Dotted records are N–S components; E–W are solid.

quality records may fail criteria 3 or 4, but produce nicely linearized signals; these results are the least robust that we retain in our study and are consequently given little weight in calculating source averages. All other records are discarded from further analysis. In all, 136 S splitting measurements are retained, 33% of our results are of A quality, 35% of B quality, and 32% are deemed C quality. The number of stations per event with splitting measurements ranges from 1 to 25. In general older earthquakes have fewer observations per earthquake, making source corrections less reliable. We calculate weighted averages on all reliable results for each event to create event specific source terms, which estimate the contribution of near-source anisotropy. These results are summarized in Table 2, Fig. 5, and Supplemental Fig. 1 in the Appendix. Source terms have delay times that range between 0.5 and 1.6 s and fast azimuths are generally parallel or sub-parallel to the trench.

As noted previously, splitting parameters do vary with incidence angle for anisotropic systems, which could mean that our S-derived source terms differ from the splitting accrued for ScS phases near the source. However without precise constraint on the actual geometry of anisotropy, it is difficult to predict the effect of take-off angle on splitting. For simple geometries (e.g. horizontal or shallowly dipping hexagonal symmetry) differences in splitting parameters with take-off angle are gradual. For the 10–15° difference in take-off angle and similar azimuths for S and ScS at a station, the differences are expected to be minor, a few tenths of a second in splitting time and a

Table 2
Source terms

Event date (mm/dd/yy)	Fast angle (°)	Delay time (s)	# S data (per event)
10/17/90	7.0	1.6	2
10/19/93	−41.0	1.2	1
1/10/94	−3.2	1.2	3
4/29/94	−34.9	1.1	4
8/19/94	−26.1	1.2	5
1/23/97	−6.5	0.9	9
7/20/97	−18.6	1.2	6
9/15/99	−35.4	1.3	11
4/23/00	2.4	0.5	3
5/12/00	−12.7	0.8	21
10/12/02	14.8	1.3	25
7/27/03	−15.0	0.9	15
3/17/04	4.5	0.8	14

degree or two in azimuth. Because our S-derived source terms are consistent with independent anisotropy analyses of the region [27] using a variety of phases, we feel confident using these results directly.

In order to assess the contribution of lowermost mantle anisotropy to ScS splitting, we use a modification of the covariance method. We search for the fast polarization and delay time that best linearizes ScS through a grid search over all azimuths, and delay times of up to 2.5 s. Prior to calculating the covariance matrix between the two orthogonal components, we correct for the previously determined source term assuming that it is the same for S and ScS. The lowermost mantle term that, combined with the calculated average source term, produces the smallest second eigenvalue maximizes particle motion linearity for each ScS arrival. It is crucial that any correction for splitting be made in the reverse order in which it was accrued. Therefore this technique effectively corrects for upper mantle anisotropy first and then any lowermost mantle contribution, before correcting for the near-source term (see Figs. 6 and 7). Results from ScS analyses are assessed using the same criteria imposed on S results. In all, we retain 57 ScS splitting measurements, 15 A, 32 B, and 10 C.

3. Results

3.1. ScS results

Results of our splitting analyses are summarized in Fig. 8. Delay times range between 0.4–2.5 s, with an average value of 1.6 s; the range is slightly lower than previous studies of the region, which have found splitting of over 4 s in a limited number of data (see Section 3.2). When plotted at the CMB bounce points, fast azimuths show a distinct spatial trend. In the south, fast azimuths are nearly orthogonal to the raypaths, suggesting SH velocities elevated relative to SV. This behavior is consistent with relatively homogenous patterns of early ScSH arrivals found in previous studies which inferred VTI. Around 5° latitude fast directions become more scattered with fast azimuths rotating counterclockwise. Above 7° latitude, fast directions are close to raypath parallel. This region corresponds to a small patch of small or negative ScSV–ScSH splits found in a previous study of the region (Supplemental Fig. 2a in the Appendix) [25]. If fast directions are closer to SV polarizations, we might expect simple peak-to-peak analyses of shear wave splitting to yield such scattered, small magnitude delay times. North of 10° latitude polarizations again become scattered, with fast directions either close to raypath parallel or nearly

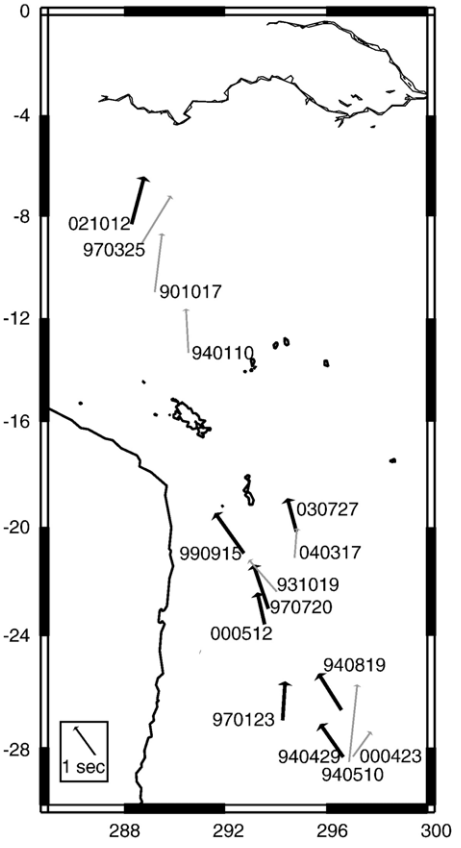

Fig. 5. Source terms plotted at the earthquake epicenter. Arrow lengths are scaled to delay time and oriented in the direction of the fast azimuth. Grey arrows indicate poorly determined source corrections. The Nazca plate subducts to the east, with the strike of the trench essentially parallel to the coastline. Note the general trend towards trench parallel fast directions.

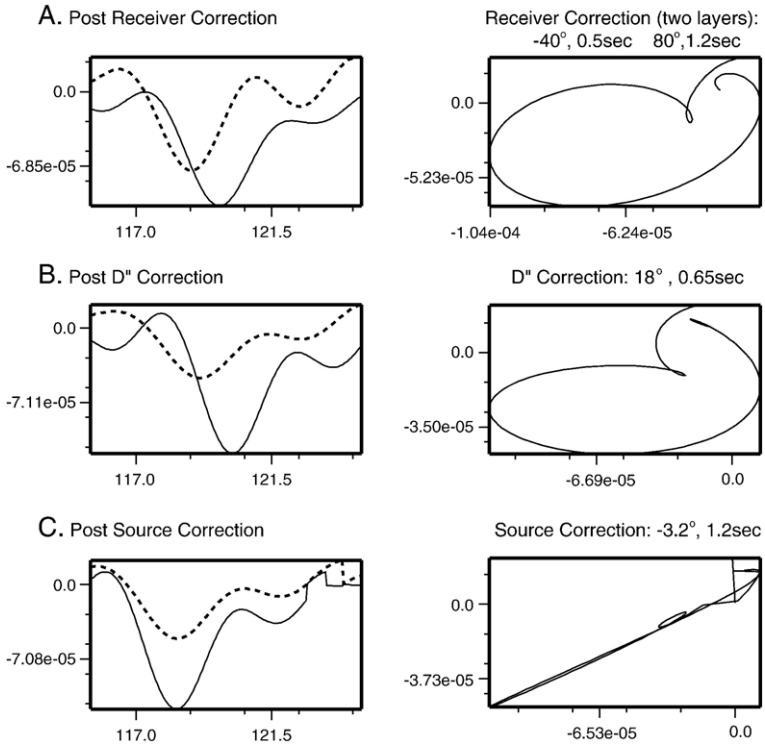

Fig. 6. Example of each correction step for an ScS waveform. This record is from station GSC from the January 10, 1994 event (see Table 1). Dotted traces are the N–S component; solid traces are the E–W component.

orthogonal. There does not appear to be a strong lateral pattern in the magnitude of delay time, but delay times in the central portion tend to be smaller than to the north or south. As with earlier work, we find no clear relationship between the regional gradient in shear wave velocity and the observed spatial trend in anisotropy. The pattern we do observe persists when only the highest quality data are plotted (Fig. 8b), suggesting that the lateral change in fast azimuths is robust.

It is difficult to fully constrain spatial trends in deep mantle anisotropy because the fairly long ScS paths in D″ limit resolution of where splitting is accrued on the deep ScS path. However, our source–receiver configuration (Fig. 2) allows for some North–South resolution; hence, plotting results at CMB bounce points gives us a sense for how splitting parameters change based on relatively small SE–NW changes in raypath. Our results could indicate the presence of a small patch of anomalous anisotropic fabric, which alters waves whose paths through D″ are dominated by it, and leaves rays that merely graze it relatively unaffected. Without the capacity to model the effect of small-scale patterns in azimuthally anisotropic structure, we cannot fully assess what mechanism of anisotropy might best explain our splitting observations. However, these results do suggest that relatively small-scale changes occur in the anisotropic fabric of D″ under the Cocos, which has important implications for dynamical models of the region. We will discuss these possibilities in further detail below.

3.2. Potential sources of error

Records from a given event show a range of fast azimuths with relative consistency for rays sampling similar paths in D″. This indicates that the lateral variations we observe are not the result of gross miscorrections for source anisotropy (Supplemental Fig. 3A in the Appendix). Splitting parameters also fail to show a consistent pattern by station, suggesting that our observations are not the result of inadequate correction for near-receiver anisotropy (Supplemental Figs. 3B and 4A in the Appendix). However, given the inherent difficulty in fully characterizing anisotropy in the upper mantle it is likely that our corrections do contain error. We have created synthetic pulses and imparted three “layers” of known splitting, in order to test the sensitivity of our results to inaccuracies in source or receiver anisotropy corrections. Our analyses are most sensitive to the last instance of splitting,

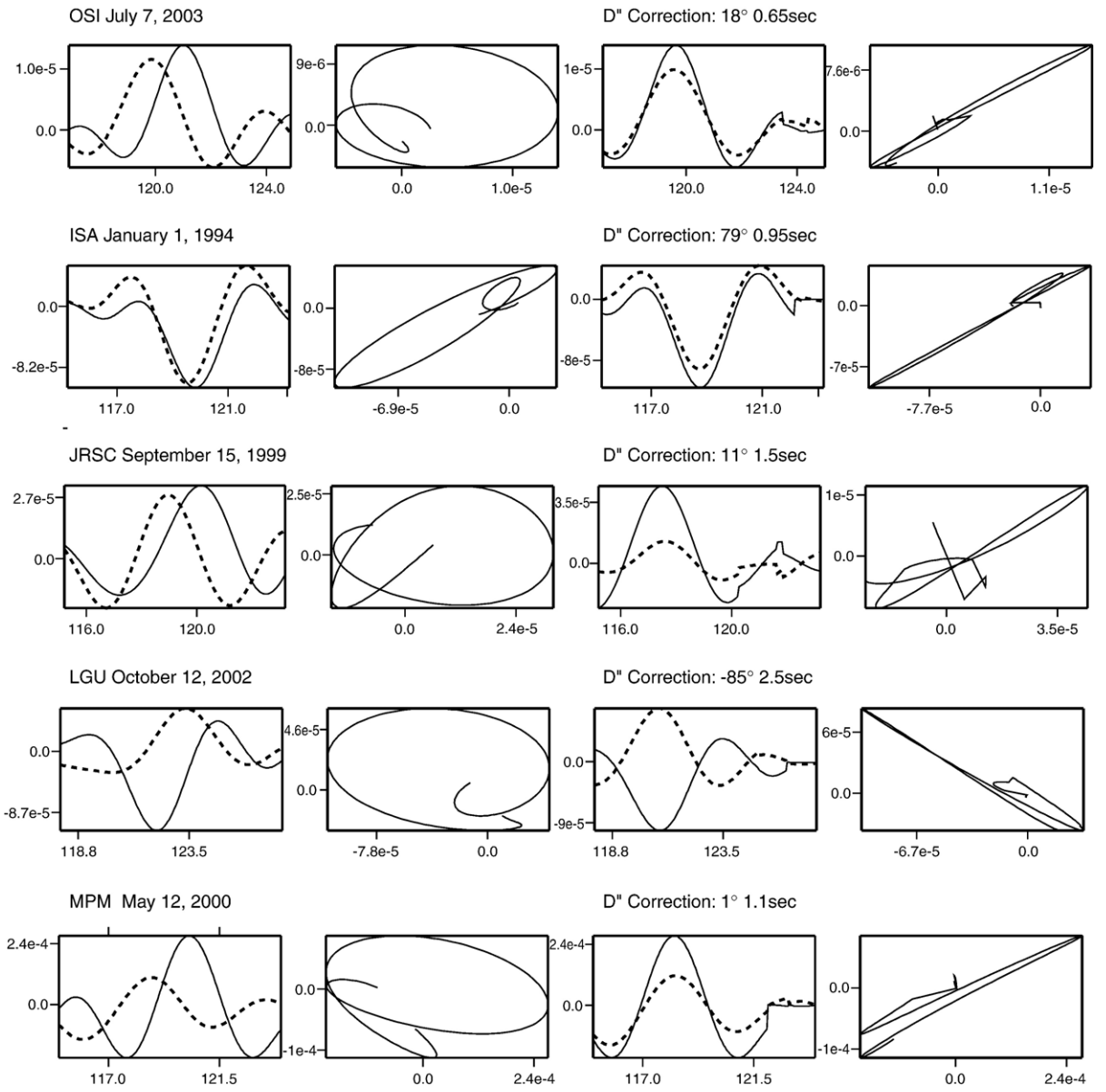

Fig. 7. More examples of ScS arrivals before and after correction for D″ and near-source anisotropy. Traces on left have been corrected for receiver-side anisotropy. Dotted traces are the N–S component; solid traces are the E–W component.

suggesting that faulty corrections for upper mantle anisotropy are most likely to alter our results. Although degenerate cases exist, under- or over-estimates of splitting parameters generally result in comparable mis-estimates of the deeper layer. We do not make an attempt to rigorously quantify these errors, however we estimate that if the upper mantle corrections we employ are within 20° and 0.5 s of the actual splitting imparted in the upper mantle, the general trend in our D″ anisotropy results will remain unaffected. Once corrections are made for near-receiver anisotropy, synthetics suggest our analyses are relatively insensitive to near-source terms. This is consistent with experience, as we have run our ScS analyses with slightly different sets of source terms (based solely on California station data or different weightings of data), as well as with no source terms, and find that the general D″ pattern remains intact (Supplemental Fig. 2B in the Appendix). However, experience with synthetics and our data both suggest that highly inaccurate source terms (more than 40° off in fast azimuth) yield unsatisfactory results. If our

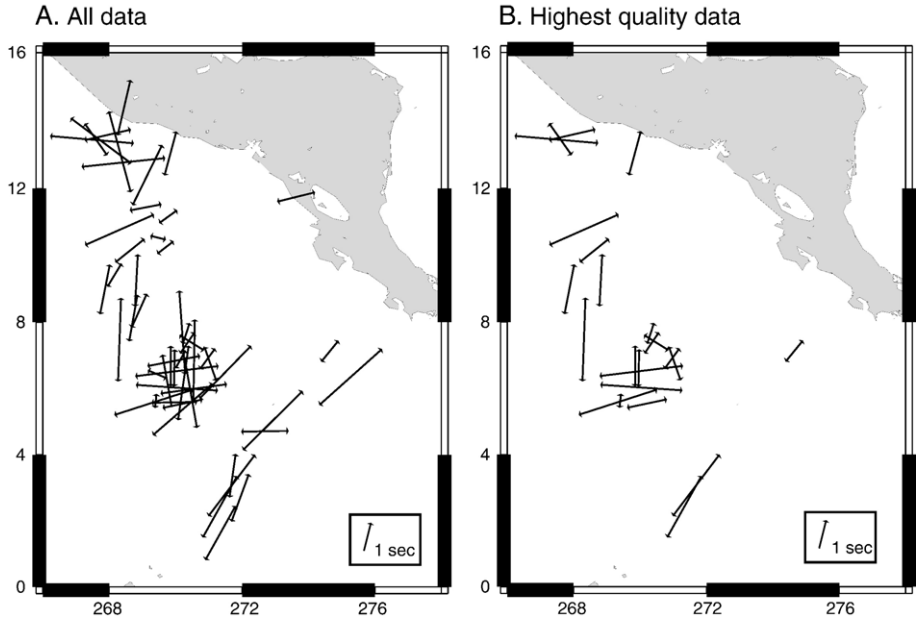

Fig. 8. Results from the ScS analyses, with source term corrections used. Arrows are scaled to delay time and oriented in the fast azimuth direction. The figure on left is all results with A, B, and C quality grades. On the right is a subset of these data, which are considered of the highest quality both in terms of source term reliability and final splitting parameter solution.

source terms bear no relation to actual near-source splitting, we might expect to see a systematic decrease in data linearization, which we do not observe. While there is some spatial coherence in the data pattern there is also overlapping scatter, which may be the result of inaccurate corrections or noise in the data. Clearly the source corrections have some uncertainty, but it is hard to ignore the S splitting and we have no clear basis to attribute it to some portion of the mantle that ScS does not traverse.

As mentioned earlier, mid-mantle anisotropy could affect our results. In particular there is the risk that we are mapping mid-mantle anisotropy into our source corrections. There is significant scatter in our S splitting measurements for some events, suggesting that residual splitting on S is not solely the result of a single source term (Supplemental Fig. 1 in the Appendix). It is difficult to fully assess this problem, but we have tested the possibility by plotting the S splitting parameters at their companion ScS bounce point (Supplemental Fig. 4B in the Appendix). This is a crude test, but if some form of regional contamination is affecting our results we might expect to see a clear spatial pattern in S residuals; no such pattern is found. If small-scale variations in anisotropic fabric exist in the mid-mantle they could affect our results, but given the lack of evidence for such behavior this possibility is difficult to constrain.

As an additional test of the robustness of our results we apply a stacking methodology to our S and ScS waveforms. For each event, we stack deconvolved waveforms of SH, SV, ScSH and ScSV to yield average wavelets. Presumably, these stacked wavelets emphasize the most robust signal, while diminishing the effect of spurious noise. These stacks are then used to determine event average S splitting parameters, which are applied in determining ScS event average splitting parameters (Supplemental Figs. 5 and 6 in the Appendix). In essence, these results give a smoothed version of our individual record results, reflecting the integrated effect of anisotropy on record populations that sample slightly different regions of D″. The source terms obtained via this method show, on average, smaller delay times than those obtained using the weighted average of individual S results. However, they are consistent with the trench parallel pattern observed in this and other studies. Although we prefer the individual record methodology detailed in the bulk of this paper, this exercise increases our confidence in the observed lateral variations in anisotropy because events that more directly sample the central region of our study area show a counterclockwise rotation of fast directions, similar to individual records with CMB bounce points in this region.

Finally, our results could be biased by the 2.5 s limit placed on the delay time by our covariance

method. Using this algorithm requires cleanly isolating the ScS phase, which means we are limited to a relatively small time window. This inherent limitation in our method could mean we are preferentially discarding large values of splitting, but this should not significantly alter our overall results given that large values of splitting, although present, are relatively limited in this region.

4. Discussion

Anisotropy at the base of the mantle could be the result of either LPO of lower mantle minerals, the alignment of inclusions or melt giving SPO, or thin, alternating layers of materials with strongly contrasting elastic properties. In this section we explore these possibilities and some notable uncertainties.

The presence of LPO would indicate a change in deformation mechanism in D″ relative to the overlying mantle. Significant increases in strain, grain size, or temperature could be enough to drive the mode of deformation into the dislocation creep regime. Numerical modeling [12,13] suggests that the strain induced by slabs descending through the lower mantle could be enough to promote strong dislocation creep in and near the slab. Although dislocation creep may be the primary mode of deformation near the slab throughout the mantle, strains might only reach threshold levels necessary for LPO formation near the CMB, thus restricting significant anisotropy to the lowermost mantle.

It may not be necessary to invoke slabs in order to create LPO, as increased temperature and lateral flow concentrated within the boundary layer might be enough to induce a change to the dislocation creep. Despite the likelihood of having large strains in D″, it remains difficult to estimate the character of anisotropy expected from LPO of lower mantle minerals. The recently discovered post-perovskite phase [14,15,45] is thought to be highly anisotropic given its layered structure, however the preferred slip planes and resulting character of anisotropy remain poorly constrained [16]. (Mg, Fe)O is also strongly anisotropic and may form fabric consistent with seismic observations (i.e. $V_{SH} > V_{SV}$) [46]. Although (Mg, Fe)O likely constitutes a small portion of the lower-mantle (20–30% by volume), it may develop strong enough anisotropy to dominate the anisotropic signature of the lowermost mantle. Most studies of perovskite indicate that it is unlikely to develop strong anisotropic fabric under lower mantle conditions and thus may be unlikely to contribute significantly to the bulk anisotropic character of D″ [6]. In general, because of the inherent difficulties in assessing the behavior of these minerals under strain at lower mantle conditions, our understanding of the preferred orientations of minerals in flow and their resulting anisotropic character remains limited. Until methods are advanced that will allow us to gain a better understanding of fabric development in the lowermost mantle it is difficult to assess whether seismologically observed anisotropy is the result of LPO.

Anisotropic structure in D″ could also result from the alignment of melt or inclusions in shear flows. Horizontally aligned disks of low velocity inclusions could effectively produce observed anisotropy, even if volume percents are low. The presence of strong shear velocity reductions in a ULVZ at the base of D″ in some regions suggests that partial melt may be present in the lowermost mantle. The stability and actual alignment of melt in horizontal (or vertical) boundary layer flow remains poorly constrained and is an important area for further research. SPO in the deep mantle may also arise from the shearing of CMB reaction products, although it is difficult to reconcile the characteristically high SH velocities in D″ with a large enough fraction of iron alloy reaction products to produce anisotropy [7]. Finally, SPO could result from velocity contrasts between low-velocity melted former crustal material and higher velocity hartzburgite mantle within a subducted slab, but only if such a slab folds and contorts extensively as it approaches and piles at the CMB [10].

In general, our results reveal variations in azimuthally anisotropic structure on a smaller length scale than previously reported in this region. This result is inconsistent with simple models of relatively homogeneous VTI. Such rapid variations in fast polarization direction have been observed previously in the Central Pacific, and were inferred to be the result of a shift from horizontal to vertical flow in the deep mantle [18]. A similar pattern of anisotropy in our study area, albeit on a smaller scale, might suggest such rapid variations in flow in the lower mantle, possibly related to small-scale upwellings (Fig. 9A) that can occur in association with the leading edge of descending slab material in D″ (e.g. [47]).

Interestingly, the region of rapid change in fast directions near 5–6° latitude (Fig. 8) corresponds to a discontinuous increase in the height of the D″ reflector above CMB, imaged using Kirchhoff migration of SH waves [28]. This correspondence suggests at a link between the topography on the discontinuity (or D″

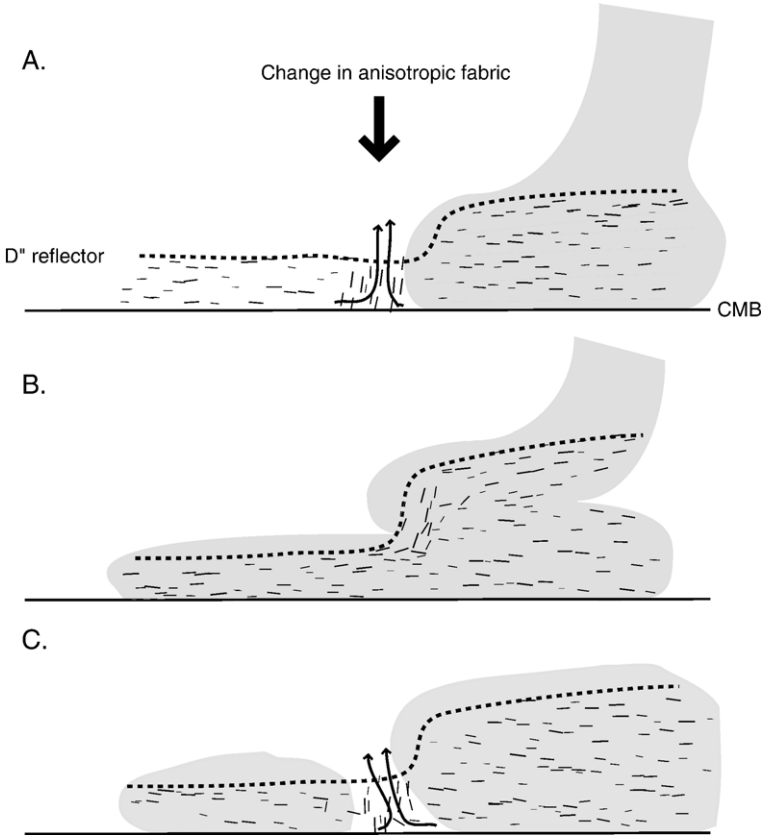

Fig. 9. Schematic representation of potential scenarios that could explain the correspondence of a step in the discontinuity with the observed pattern of anisotropy. A small region of anisotropic fabric exhibiting fast directions parallel to the raypath could arise from (A) a limited patch of upwelling near the margin of a downwelling slab; (B) vertical orientation of inherent anisotropic fabric in a folded slab impinging on the CMB; or (C) complexity related to intense chemical heterogeneity.

thickness) and the anisotropic fabric. Previous studies in the region have suggested that the onset of splitting with depth is coincident with the discontinuity, strengthening this connection. The scenario illustrated in Fig. 9A, could also result in a step in the D″ reflector if such a feature is related to the transition from perovskite to post-perovskite (with the transition elevated in the colder near-slab region). Similarly, Hutko et al. [28] propose that this apparent step in the discontinuity may be related to folding in a recumbent slab lying on the CMB, with post-perovskite in the cold slab material producing the discontinuity. Given this scenario, it is possible that the anisotropic fabric within the slab is re-oriented where the actual bend occurs, possibly due to the dynamic bending of the slab material, creating a limited region in which ScSV travels faster than ScSH (Fig. 9B). It is also possible that strong chemical heterogeneity is responsible for the complexities in D″ beneath the Cocos (Fig. 9C). Present or past flow between regions with different chemical signatures could lead to complex patterns of anisotropy, but this scenario is almost unconstrained.

Although these scenarios are speculative, our results do have several important implications for models of the deep mantle. The apparent azimuthal anisotropy in the region suggests that models of the lowermost mantle need not be limited to structures and fabric which give rise to VTI-like behavior. For example, scenarios dependent on LPO of MgO or perovskite have often been discarded based on the difficulty in finding orientations which produces behavior consistent with VTI, but the presence of azimuthal anisotropy makes such barriers moot. More importantly, the rapid change in fast azimuths observed over the lateral extent of our study area suggests that the region is dynamic enough to produce changes in the anisotropic fabric over length scales of less than 200 km. This could suggest the existence of complicated strain fields due to the downwelling and spreading out of slab material, complex patterns of

boundary layer flow, and/or intense chemical heterogeneity.

The significant near-source anisotropy isolated in this study suggests that ignoring this contribution may result in the mischaracterization of D″ anisotropy. Garnero et al. [22] and Maupin et al. [23] use full waveform synthetics to model a positive upswing on expected negative polarity SV components of S and Sdiff waveforms sampling D″ beneath the Cocos, finding an SE–NW trend in azimuthal anisotropy. Many of the sources used in this study overlap with our own, however near-source anisotropy was neglected. In order to test the sensitivity of these waveforms to near-source anisotropy, we have made corrections for the appropriate source terms for a sampling of the Maupin et al. dataset. After applying the source term corrections, the SV upswings were reduced for some of the data. If some form of azimuthal anisotropy does exist in D″, as our results suggest, correcting the waveforms in this order is not strictly correct. However, the results of these tests do indicate that near-source anisotropy alters the character of the modeled upswing and thus, may have a significant effect on the inferred pattern of D″ anisotropy. Future work must address the near-source effects on all studies of lower mantle anisotropy, as noted by Wookey et al. [31].

5. Conclusions

Shear wave splitting analyses reveal the presence of azimuthal anisotropy in D″ beneath the Cocos plate. Rapid lateral variations in fast azimuths suggest that anisotropic fabric changes over a small length scale (~200 km). Past work has emphasized the contrast between fairly homogenous anisotropy inferred for high velocity D″ regions and the more intense variability observed in low velocity areas; taken together our results suggest that the anisotropic character of these D″ regions may not be as distinct as previously suggested. A geographical correlation between the onset of variable anisotropy and previously imaged topography of the D″ discontinuity gives supporting evidence for a connection between these two phenomena.

This characterization of azimuthal anisotropy beneath the Cocos Plate has important implications for work on anisotropy in other regions of the earth. Many studies of upper mantle anisotropy utilize SKS waves under the assumption that D″ is dominated by VTI, which should have little affect on nearly vertical SKS waves. If azimuthal anisotropy is significant in regions of D″, as our work suggests, the assumption that SKS is not contaminated by lower mantle anisotropy becomes difficult to justify.

Our method for isolating the signature of D″ anisotropy appears to enhance coherence within our data, which suggests it may be useful in shear-wave splitting analyses of other, more complicated regions of D″. In general, our S wave splitting analyses further strengthens the argument that near-source contamination must be taken into account when studying deep mantle anisotropy.

Acknowledgements

We thank Martha Savage for a thoughtful review. We obtained data from the BDSN, TRInet and IRIS data centers. We thank Renate Hartog for the anisotropy analysis software. This research was supported by the NSF grant EAR-0125595 (TL and JR), and EAR-0135119 (EJG); contribution 491 of the Center for the Studies of Imaging and Dynamics of the Earth.

Appendix A. Supplementary data

Supplementary data associated with this article can be found, in the online version, at doi:10.1016/j.epsl.2006.06.005.

References

[1] T. Lay, E.J. Garnero, Core–mantle boundary structures and processes, in: R.S.J. Sparks, C.J. Hawkesworth (Eds.), The State of the Planet: Frontiers and Challenges in Geophysics, Geophysical Monograph, vol. 150, IUGG, 2004, pp. 1–17, Volume 19.

[2] E.J. Garnero, Heterogeneity of the lowermost mantle, Annu. Rev. Earth Planet. Sci. 28 (2000) 509–537.

[3] T. Lay, E.J. Garnero, Q. Williams, Partial melting in a thermo-chemical boundary layer at the base of the mantle, Phys. Earth Planet. Inter. 146 (2004) 441–467.

[4] P.G. Silver, Seismic anisotropy beneath the continents: probing the depths of geology, Annu. Rev. Earth Planet. Sci. 24 (1996) 385–432.

[5] M.K. Savage, Seismic anisotropy and mantle deformation: What have we learned from shear wave splitting? Rev. Geophys. 37 (1999) 65–106.

[6] S.I. Karato, Some remarks on the origin of seismic anisotropy in the D″ layer, Earth Planets Space 50 (1998) 1019–1028.

[7] J.-M. Kendall, P.G. Silver, Investigating Cause of D″ anisotropy, in: M. Gurnis, M. Wysession, E. Knittle, B. Buffett (Eds.), The Core–Mantle Boundary Region, Geodyn. Ser., vol. 28, AGU, Washington D.C., 1998, pp. 97–118.

[8] T. Lay, E.J. Garnero, Q. Williams, L. Kellogg, M.E. Wysession, Seismic wave anisotropy in the D″ region and its implications, in:

M. Gurnis, M. Wysession, E. Knittle, B. Buffett (Eds.), The Core–Mantle Boundary Region, AGU, Washington, D.C., 1998, pp. 299–318.

[9] J.-M. Kendall, Seismic anisotropy in the boundary layers of the mantle, in: S. Karato, A.M. Forte, R.C. Liebermann, G. Masters, L. Stixrude (Eds.), Earth's Deep Interior: Mineral Physics and Tomography from the Atomic to the Global Scale, 2000, pp. 133–159.

[10] M.M. Moore, E.J. Garnero, T. Lay, Q. Williams, Shear wave splitting and waveform complexity for lowermost mantle structures with low-velocity lamellae and transverse isotropy, J. Geophys. Res. 109 (2004) B02319, doi:10.1029/2003jb002546.

[11] C. Meade, P.G. Silver, S. Kaneshima, Laboratory and seismological observations of lower mantle isotropy, Geophys. Res. Lett. 22 (1995) 1293–1296.

[12] A.K. McNamara, P.E. van Keken, S. Karato, Development of anisotropic structure in the Earth's lower mantle by solid-state convection, Nature 416 (2002) 1136–1139.

[13] A.K. McNamara, P.E. van Keken, S. Karato, Development of finite strain in the convecting lower mantle and its implications for seismic anisotropy, J. Geophys. Res. 108 (2003) B07402, doi:10.1029/2003JB002847.

[14] M. Murakami, K. Hirose, K. Kawamura, N. Sata, Y. Ohishi, Post-perovskite phase transition in $MgSiO_3$, Science 304 (2004) 855–858.

[15] T. Iitaka, K. Hirose, K. Kawamura, M. Murakami, The elasticity of the MgSiO3 post-perovskite phase in the Earth's lowermost mantle, Nature 430 (2004) 442–445.

[16] S. Stackhouse, J.P. Brodholt, J. Wookey, J.M. Kendall, G.D. Price, The effect of temperature on the acoustic anisotropy of the perovskite and post-perovskite polymorphs of MgSiO3, Earth Planet. Sci. Lett. 230 (2005) 1–10.

[17] S. Merkel, A. Kubo, L. Miyagi, S. Speziale, T.S. Duffy, H.K. Moo, H.R. Wenk, Plastic deformation of $MgGeO_3$ post perovskite at lower mantle pressures, Science 311 (2006) 644–646.

[18] S.A. Russell, T. Lay, E.J. Garnero, Small-scale lateral shear velocity and anisotropy near the core–mantle boundary beneath the central Pacific imaged using broadband ScS Waves, J. Geophys. Res. 104 (1999) 13,183–13,199.

[19] S.R. Ford, E.J. Garnero, A.K. McNamara, A strong lateral shear velocity gradient and anisotropy heterogeneity in the lowermost mantle beneath the southern Pacific, J. Geophys. Res. 111 (2005), doi:10.1029/2004JB003574.

[20] S.A. Russell, C. Reasoner, T. Lay, K. Revenaugh, Coexisting shear- and compressional-wave seismic velocity discontinuities beneath the central Pacific, Geophys. Res. Lett. 28 (2001) 2281–2284.

[21] E.J. Garnero, M.M. Moore, T. Lay, M. Fouch, Isotropy or weak vertical transverse isotropy in D″ beneath the Atlantic Ocean, J. Geophys. Res. 109 (2004), doi:10.1029/2004JB003004.

[22] E.J. Garnero, V. Maupin, T. Lay, M. Fouch, Variable azimuthal anisotropy in Earth's lowermost mantle, Science 306 (2004) 259–261.

[23] V. Maupin, E.J. Garnero, T. Lay, M.J. Fouch, Azimuthal anisotropy in the D″ layer beneath the Caribbean, J. Geophys. Res. 110 (2005) B08301, doi:10.1029/2004JB003506.

[24] E.J. Garnero, T. Lay, D″ shear velocity heterogeneity, anisotropy and discontinuity structure beneath the Caribbean and Central America, Phys. Earth Planet. Inter. 140 (2003) 219–242.

[25] J.M. Rokosky, T. Lay, E.J. Garnero, S.A. Russell, High-resolution investigation of shear wave anisotropy in D″ beneath the Cocos Plate, Geophys. Res. Lett. 31 (2004) L07605, doi:10.1029/2003GL018902.

[26] C. Thomas, E.J. Garnero, T. Lay, High-resolution imaging of lowermost mantle structure under the Cocos Plate, J. Geophys. Res. 109 (2004), doi:10.1029/2004JB003013.

[27] T. Lay, E.J. Garnero, S.A. Russell, Lateral variation in the D″ discontinuity beneath the Cocos Plate, Geophys. Res. Lett. 31 (2004), doi:10.1029/2004GL020300.

[28] A.R. Hutko, T. Lay, E.J. Garnero, J.S. Revenaugh, Seismic detection of folded, subducted lithosphere at the core–mantle boundary, Nature 441 (2006) 333–336.

[29] R.M. Russo, P.G. Silver, Trench-parallel flow beneath the Nazca plate from seismic anisotropy, Science 264 (1994) 1105–1111.

[30] M.L. Anderson, G. Zandt, E. Triep, M. Fouch, S. Beck, Anisotropy and mantle flow in the Chile–Argentina subduction zone from shear wave splitting analysis, Geophy. Res. Lett. 31 (2004) L23608, doi:10.1029/2004GL020906.

[31] J. Wookey, J.-M. Kendall, G. Rümpker, Lowermost mantle anisotropy beneath the north Pacific from differential S–ScS splitting, Geophys, J. Int. 161 (3) (2005) 829–838.

[32] M. Bostock, J.F. Cassidy, Variations in SKS splitting across western Canada, Geophys. Res. Lett. 22 (1995) 5–8.

[33] G. Barruol, P.G. Silver, Seismic anisotropy in the eastern United States: deep structure of a complex continental plate, J. Geophys. Res. 102 (1997) 8329–8348.

[34] J. Polet, H. Kanamori, Anisotropy beneath California: shear wave splitting measurements using a dense broadband array, Geophys. J. Int. 149 (2002) 313–327.

[35] C.A. Currie, J.F. Cassidy, R.D. Hyndman, M.G. Bostock, Shear wave anisotropy beneath the Cascadia subduction zone and western North American craton, Geophys. J. Int. 157 (2004) 341–353.

[36] R. Hartog, S.Y. Schwartz, Subduction-induced strain in the upper mantle east of the Mendocino triple junction, California, J. Geophys. Res. 105 (2000) 7907–7930.

[37] R. Hartog, S.Y. Schwartz, Depth-dependent mantle anisotropy below the San Andreas fault system: apparent splitting parameters and waveforms, J. Geophys. Res. 106 (2001) 4155–4167.

[38] S. Özalaybey, M.K. Savage, Shear-wave splitting beneath western United States in relation to plate tectonics, J. Geophys. Res. 100 (1995) 18,135–118,149.

[39] E.J. Garnero, T. Lay, Lateral variations in lowermost mantle shear wave anisotropy beneath the north Pacific and Alaska, J. Geophys. Res. 102 (1997) 8121–8135.

[40] J. Trampert, H.J. van Heijst, Global azimuthal anisotropy in the transition zone, Science 296 (2002) 1297–1299.

[41] W.-P. Chen, M.R. Brudzinski, Seismic anisotropy in the mantle transition zone beneath Fiji–Tonga, Geophys. Res. Lett. 30 (2003), doi:10.1029/2002GL016330.

[42] J. Wookey, J-M. Kendall, Evidence of mid-mantle anisotropy from shear wave splitting and the influence of shear coupled P-waves, J. Geophys. Res. 109 (2004) B07309, doi:10.1029/2003JB002871.

[43] P.G. Silver, W.W. Chan, Shear-wave splitting and subcontinental mantle deformation, J. Geophys. Res. 96 (1991) 16,429–16,454.

[44] G. Ekström, A.M. Dziewonski, N.N. Maternovskaya, M. Nettles, Phys. Earth Planet. Inter. 148 (2005) 327–351.

[45] T. Lay, D. Heinz, M. Ishii, S.-H. Shim, J. Tsuchiya, T. Tsuchiya, R. Wentzcovitch, D. Yuen, Multidisciplinary impact of the deep mantle phase transition in perovskite structure, EOS 86 (2005) 1–3.
[46] D. Yamazaki, S. Karato, Fabric development in (Mg, Fe)O during large strain, shear deformation: implications for seismic anisotropy in Earth's lower mantle, Phys. Earth Planet. Inter. 131 (2002) 251–267.
[47] E. Tan, M. Gurnis, L. Han, Slabs in the lower mantle and their modulation of plume formation, Geochem. Geophys. Geosyst. 3 (11) (2002), doi:10.1029/2001GC000238.